nature portfolio

Peer Review File

Microporous Membrane with Ionized Sub-nanochannels Enabling Highly Selective Monovalent and Divalent Anion Separation

Reviewers' Comments:

Reviewer #1:
Remarks to the Author:
The authors fabricated a microporous polymer membrane featuring an ionized sub-nanochannel and investigated the ionic transportation behavior of the membrane. The results indicated that the membranes exhibited outstanding separation performance between Cl- and SO42-/CO32-. The authors elucidated the ion separation mechanism effectively through characterization and DFT calculation. These findings provide interesting new ideas for ion exchange membrane materials and theories in desalination and ion separation. Overall, this manuscript meets the standards for publication in Nature Communications. Before accepting this manuscript, the following concerns need to be addressed.
1. Clarification is needed on the differing migration tendencies of chloride ions and carbonate ions as observed in Fig. 4c.
2. Does quaternization affect the structure of TB membranes? Are defects likely to occur?
3. Could you please provide an explanation to why the low adsorption and desorption of CO2 in the BET test. Why wasn't N2 used for testing?
4. “However, the absence of ioninteracting groups within the sub-nanochannel increases the energy barrier of anion entry, resulting in a reciprocal relationship between anion selectivity.” Clarification is needed on this statement regarding the absence of ion-interacting groups within the sub-nanochannel leading to an energy barrier increase for anion entry and its reciprocal relationship with anion selectivity.
5. In Fig. 4d, the comparison of performance of Cl- and SO42- is made but Fig. 4 mainly show separation between Cl- and CO32-. Although this comparison is equally important, it may be slight misleading to the readers. Suggest to either include the comparison for Cl- and CO32- or to include similar performance characterisation for Cl- and SO42- in Fig. 4. Please also avoid comparing both Cl- and CO32- and Cl- and SO42- in Fig. 4d as all datapoints are for Cl- and SO42-, and plotting data point for Cl- and CO32- has little incentive.
6. “The bright regions represent the hydrophobic segments of the polymer backbone, whereas the dark regions correspond to the hydrophilic portions of the quaternary ammonium group” Could the author explain this further? i.e., how is the difference in peak and valley related to the different segments of the polymer backbone?
7. Authors should review the entire manuscript to ensure proper formatting, including journal name abbreviations, subscripts, and superscripts in the figures etc. “The effective area of the membrane inside the device was 19.625 cm2. Please also ensure the right significant figure is used.

Reviewer #2:
Remarks to the Author:
The authors discuss the synthesis, membrane preparation and application of ionized sub-nanochannels for ion sieving. The research is new and interesting, of interest to a broad audience. In general, it is well-written and easy to follow, the characterizations are detailed. I recommend publication after addressing the comments below.

1. The size of the hydrophilic-hydrophobic nanodomains should be indicated in the figure showing the Tröger's base microporous polymer membrane schematic.
2. The used monomers are sterically hindered near the reaction site, which usually prevents the polymerization or reduces the yield. The authors could elaborate on these aspects more and discuss how these obstacles were overcome.
3. The radar plot is somewhat difficult to read and therefore the data presented could be also included in the supporting information in a tabulated form.
4. The degree of methylation as well as the molecular weight of the polymer should be determined because it is an important factor influencing the membrane performance.
5. The ion separation performance of the membranes should be compared with the state of the art membranes in the literature.

Reviewer #3:
Remarks to the Author:
This study introduced randomly twisted V-shaped Tröger's Base units and quaternary ammonium groups to construct ionized sub-nanochannel membranes. By combining size sieving and electrostatic interactions, the membranes demonstrated impressive selectivity for separating monovalent and divalent anions. The results represent significant breakthroughs and have broad interest, with a comprehensive and reasonable separation mechanism. Therefore, the study is suitable for publication in Nature Communications with minor revisions suggested. Specific comments are listed below:

1. The authors proposed in the abstract section that the V-shaped structure of TB unit with quaternary ammonium groups constructs ionized sub-nanochannels. Polymer membranes are usually described as possessing ion channels or transport channels, so the authors could describe in detail what is meant by ionized sub-nanochannels.
2. “Although a minimal migration of CO32- was observed within the final 35 minutes, amounting to less than one-fifth of the migration of Cl-, it remained relatively steady (Fig. 3b).” This is an interesting experimental phenomenon. Are there any potential reasons that the authors could provide?
3. “The migration of Cl- in one hour was markedly higher than that of SO42- (Supplementary Fig. 7), achieving a Cl- flux of 20.37 × 10-4 mol m-2 s-1 and a permeation selectivity of 82 (Supplementary Fig. 8). The ion migration rate was even faster than that in the Cl-/CO32- system, with complete Cl- migration achieved within 48 hours (Supplementary Fig. 9), while the optimal permeation selectivity was slightly lower.” In this article, the membrane constructed all showed high ion fluxes and permeation selectivity in the ion separation process. Why the ion flux is lower in the Cl-/CO32- system but the selectivity is higher?
4. “However, the Cl- and SO42- separation performance of the QA-TB membrane far exceeded those reported in the literature (Fig. 4e).” The authors compared the performance of the fabricated membranes with data from seven references. Suggesting the authors to compare the data with more literature.
5. “Meanwhile, different degrees of interaction between the QA-TB framework and ions help ions

with different free energies and transfer along the pore walls at different speeds.” What does “interaction” mean? Please give a specific explanation.

Response to Reviewers' Comments

Thank you for constructive comments from the reviewers. We responded the comments from the reviewers (original reviewers comments marked in black and our response in blue color) and highlighted the changes in italic characters in these responses and marked in blue color in the main text

Response to Reviewer #1

General Comment: The authors fabricated a microporous polymer membrane featuring an ionized sub-nanochannel and investigated the ionic transportation behavior of the membrane. The results indicated that the membranes exhibited outstanding separation performance between Cl^- and SO_4^{2-}/CO_3^{2-}. The authors elucidated the ion separation mechanism effectively through characterization and DFT calculation. These findings provide interesting new ideas for ion exchange membrane materials and theories in desalination and ion separation. Overall, this manuscript meets the standards for publication in Nature Communications. Before accepting this manuscript, the following concerns need to be addressed.

Our response to General Comment

We appreciate the reviewer's careful evaluation of our work. According to your thoughtful and valuable suggestions, we have made the relevant modifications to improve the quality of the manuscript as shown below:

Comment #1

Clarification is needed on the differing migration tendencies of chloride ions and carbonate ions as observed in Fig. 4c.

Our response to Comment #1

Thank you for your suggestion. There is a difference between the size and hydration free energy of chloride ions and carbonate ions, which could affect the dehydration and migration of these ions. At the same time, the degree of electrostatic interaction between the ions and the quaternary ammonium groups of the QA-TB membrane is different, resulting in different migration tendencies of the ions. The size and hydration free energy of chloride ions are smaller, and the adsorption and desorption energy between chloride ions and QA-TB is also smaller, so chloride ions can dehydrate and migrate quickly, resulting in an increase in their migration amount. The size and hydration energy of the carbonate ions are larger than chloride ions. They are more difficult to desorb compared with chloride ions. Therefore, the migration rate is extremely lower, and the migration amount is less if we compare these two ions. We described the differing migration tendencies and analyzed the explanations as follows:

Unveiling separation mechanisms.

(main text, page 12) '*As a result, the migration amount of* Cl^- *in the concentration chamber steadily increased over 12 days until it plateaued due to complete migration of* Cl^- *in the dilution chamber, whereas the slow penetration of* CO_3^{2-} *resulted in its migration remaining minimal and plateaued (**Fig. 4c**).*'

Comment #2

Does quaternization affect the structure of TB membranes? Are defects likely to occur?

Our response to Comment #2

Thank you for your comment. Quaternization enhances the interaction between polymer chains and reduce the membrane pores. However, no defects were found. In the revised manuscript, SEM was used to observe the microstructure of the membrane surface as can be seen in a new Supplementary Figure 5 (see below). It was found that the TB and QA-TB membranes have the characteristic surface of dense polymer membranes without obvious defects. Moreover, the generation of defects is bound to affect the separation performance of the membrane. In **Fig. 4c**, the long-term separation performance of ions is stable, which indirectly indicates the integrity of the membrane structure.

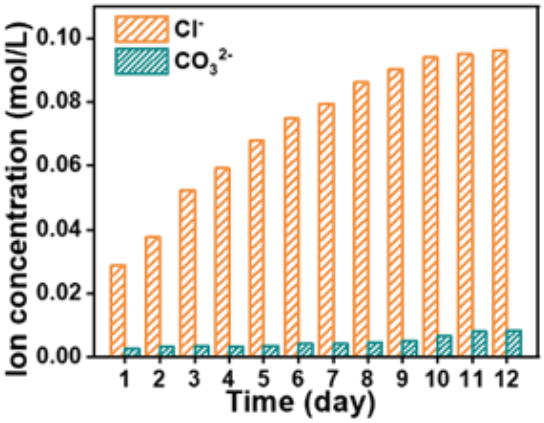

Fig. 4c Ion concentration in the concentration chamber.

We have stated the integrity of the membrane structure in the *main text* and *SI*, respectively.

(main text, page 6) '*The structural composition of the TB units and the incorporation of QA groups give TB/QA-TB membranes distinctive and superior physical and chemical properties. The membranes have the characteristic surface of dense polymer membranes without obvious defects (**Supplementary Fig. 5**).*'

(SI, page 3) '*The morphology of membranes was observed by a field emission*

scanning electron microscope (FESEM, Hitachi S4800). Before observation, the membranes were freeze-dried to remove residual water and then coated with a thin layer of gold nanoparticles.'

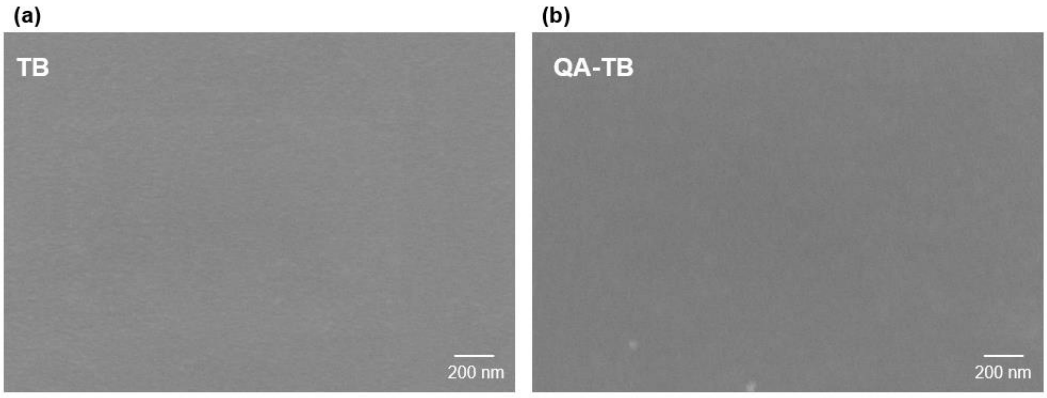

Supplementary Fig. 5 *Surface morphologies of (a) TB and (b) QA-TB membranes.*

Comment #3

Could you please provide an explanation to why the low adsorption and desorption of CO2 in the BET test. Why wasn't N_2 used for testing?

Our response to Comment #3

Thank you for your suggestion. The decrease in CO_2 adsorption on the QA-TB membrane is due to the quaternary ammonium modification, which narrows the membrane pores. Additionally, the introduced ammonium cations and iodine anions hinder CO_2 adsorption, resulting in low adsorption. According to the reviewer's suggestion, we added the N_2 adsorption curve in the SI. However, the results showed a lower adsorption amount. This is because CO_2 is mainly used to test micropores smaller than 2 nm, while N_2 tests mesopores or macropores. The pore sizes of the TB and QA-TB membranes in this study are both less than 1 nm. CO_2, being smaller, diffuses faster and reaches saturated adsorption more easily compared to N_2. We have supplemented the N_2 test in *SI* and added the following instructions:

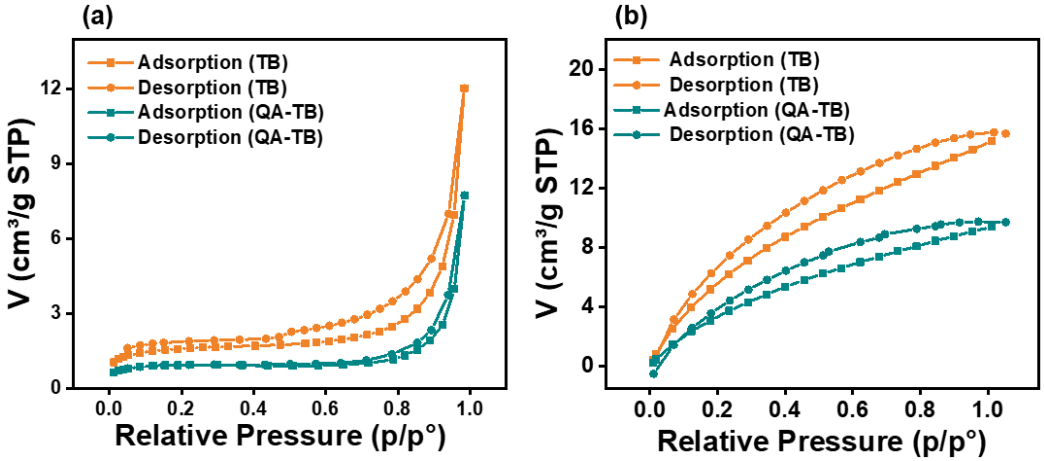

Supplementary Fig. 15 *(a) N_2 and (b) CO_2 adsorption/desorption curve of the TB/QA-TB membrane.*

Note: CO_2 is primarily used to probe microporous pores smaller than 2 nm, while N_2 is mainly used to test mesopores or macropores. Due to its smaller size and faster diffusion rate compared to N_2, CO_2 more easily reaches saturated adsorption. PALS results indicate that the TB and QA-TB in this work have pore sizes less than 1 nm, classifying them as microporous structures. Consequently, N_2 adsorption is lower than that of CO_2. Additionally, compared to the TB membrane, the reduced adsorption on the QA-TB membrane is due to the quaternary ammonium modification, which strengthens ion/polar chain interactions, resulting in narrower membrane pores.

Comment #4

"However, the absence of ion-interacting groups within the sub-nanochannel increases the energy barrier of anion entry, resulting in a reciprocal relationship between anion selectivity." Clarification is needed on this statement regarding the absence of ion-interacting groups within the sub-nanochannel leading to an energy barrier increase for anion entry and its reciprocal relationship with anion selectivity.

Our response to Comment #4

Thank you for your rigorous and responsible comment. In this sentence, we lost the word 'conductivity'. The absence of ion-interacting groups within the sub-nanochannel increases the energy barrier of anion entry, resulting in a reciprocal relationship between anion **selectivity** and **conductivity**, which we have supplemented in the *main text*.

(main text, page 4) '*However, the absence of ion-interacting groups within the sub-nanochannel increases the energy barrier of anion entry, resulting in a reciprocal relationship between anion selectivity and conductivity*.'

Comment #5

In Fig. 4d, the comparison of performance of Cl^- and SO_4^{2-} is made but Fig. 4 mainly show separation between Cl^- and CO_3^{2-}. Although this comparison is equally important, it may be slight misleading to the readers. Suggest to either include the comparison for Cl^- and CO_3^{2-} or to include similar performance characterisation for Cl^- and SO_4^{2-} in Fig. 4. Please also avoid comparing both Cl^- and CO_3^{2-} and Cl^- and SO_4^{2-} in Fig. 4d as all datapoints are for Cl^- and SO_4^{2-}, and plotting data point for Cl^- and CO_3^{2-} has little incentive.

Our response to Comment #5

Thank you for your suggestion. Due to the similar physical and chemical properties of Cl^- and CO_3^{2-}, their effective separation is challenging. There are few literature reports on the separation of these two ions. To facilitate readers' understanding, we have replaced the performance comparison chart with data on the separation of various monovalent/divalent anions (**Fig. 4e**). A table listing specific data and ion types has been added to the SI, along with the latest published literature data (**Supplementary Table 3**).

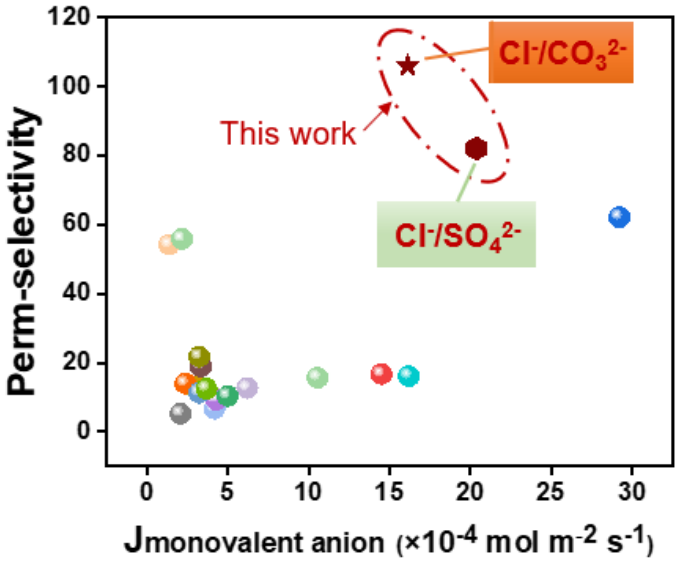

Fig. 4e *Comparison of monovalent and divalent anion separation performance of QA-TB membrane with previously reported membranes.*

Supplementary Table 3 *Comparison of monovalent and divalent anion separation performance of QA-TB membrane with previously reported membranes.*

Type of membranes	Separation system	Monovalent anion flux ($\times 10^{-4}$ mol m^{-2} s^{-1})	Permeation selectivity	Reference
PAES-UIO-66-Pyr	Cl^-/SO_4^{2-}	1.4	54.26	16
QDPAB-C7	Cl^-/SO_4^{2-}	10.56	15.7	17
HPABP-CC3(15)	Cl^-/SO_4^{2-}	6.22	12.67	18
QP-P3-1	Cl^-/SO_4^{2-}	4.2	6.7	19
QP-P6-1	Cl^-/SO_4^{2-}	4.3	9.3	19
QP-P11-1	Cl^-/SO_4^{2-}	3	13.07	19
PPO-0.100-ImPS	Cl^-/SO_4^{2-}	16.2	16.12	20
sCOF/aAEM3	Cl^-/SO_4^{2-}	3.35	18.92	21
Blend-15 AIEM	Cl^-/SO_4^{2-}	3.25	21.8	22
Blend-10 AIEM	Cl^-/SO_4^{2-}	2.4	14	22
Blend-0 AIEM	Cl^-/SO_4^{2-}	3.25	11.3	22
PAES-im-2.5c AIEM	Cl^-/SO_4^{2-}	3.7	12.5	23
Neosepta ACS	Cl^-/SO_4^{2-}	2.1	5.27	23
MQ18	Cl^-/SO_4^{2-}	14.5	16.7	24
AF1-HNN5-50	Cl^-/SO_4^{2-}	29.2	62.2	25
PQC76/DSA-0.5	Cl^-/SO_4^{2-}	5	10.38	26
PAES-UIO-66-Py	NO_3^-/SO_4^{2-}	2.19	55.9	16
QA-TB	Cl^-/SO_4^{2-}	20.37	82	This work
QA-TB	Cl^-/CO_3^{2-}	16.13	106	This work

Comment #6

"The bright regions represent the hydrophobic segments of the polymer backbone, whereas the dark regions correspond to the hydrophilic portions of the quaternary ammonium group" Could the author explain this further? i.e., how is the difference in peak and valley related to the different segments of the polymer backbone?

Our response to Comment #6

Thank you for your comment. Peak and valley in AFM images represent the roughness of the surface of the membranes as the principle of AFM is using tapping mode of the

needles. When casting ionic polymers on the glass plate, film surface is exposed to the air, whereas the bottom side is toward the glass plate. Air is hydrophobic and the glass plate is regarded as hydrophilic. After casting, hydrophobic chains migrate toward the air side of the surface, resulting in hydrophobic bright regions in the valley part. Or as the needle in AFM taps the surface of the membrane, hard and hydrophobic aromatic groups are more rigid than the flexible soft and hydrophilic regions in QA-TB, therefore peak regions appear in dark regions and vice versa. Therefore, the bright regions represent the hydrophobic segments of the polymer backbone, whereas the dark regions correspond to the hydrophilic portions of the quaternary ammonium groups. Obviously, ionic polymers like QA-TB have both hydrophilic and hydrophobic characters. The main chain of the polymers is hydrophobic, whereas the quaternary ammonium group is hydrophilic. This hydrophilicity and hydrophobicity difference leads to a microphase separation morphology in the polymer film, observable as bright and dark areas in the AFM. This is illustrated in **Fig. 6c.** We have added the explanation in the main text and Supplementary Methods, as follows:

(main text, pages 16-17) '*In contrast, the QA-TB membrane displays distinct light and dark regions due to the different hydrophilicity of the polymer and functional groups. The bright regions represent the hydrophobic segments of the polymer backbone, whereas the dark regions correspond to the hydrophilic portions of the quaternary ammonium groups.*'

(SI, pages 3) '*Peak and valley in AFM images represent the roughness of the surface of the membranes as the principle of AFM is using tapping mode of the needles. When casting ionic polymers on the glass plate, film surface is exposed to the air, whereas the bottom side is toward the glass plate. Air is hydrophobic and the glass plate is regarded as hydrophilic. After casting, hydrophobic chains migrate toward the air side of the surface, resulting in hydrophobic bright regions in the valley part. Additionally, as the needle in AFM taps the surface of the membrane, hard and hydrophobic groups are more rigid than the flexible soft and hydrophilic regions, therefore peak regions appear in dark regions and vice versa. Therefore, the bright regions represent the hydrophobic segments of the polymer backbone, whereas the dark regions correspond to the hydrophilic portions.'*

Comment #7

Authors should review the entire manuscript to ensure proper formatting, including journal name abbreviations, subscripts, and superscripts in the figures etc. "The effective area of the membrane inside the device was 19.625 cm^2. Please also ensure the right significant figure is used.

Our response to Comment #7

Thank you for your rigorous and responsible comment. We have checked the spelling

and format of the manuscript again. The following revisions were made:

(main text, Page 9) '*The effective area of the membrane inside the device was **19.63** cm^2.*'

(main text, Page 20) '*Each test assessed one anionic membrane and two cationic membranes, striking a balance between the concentration pressure difference of the system where the testing area of each membrane in the device spanned **19.63** cm^2.*'

(references, Page 23) '*Liang Y, Zhu Y, Liu C, Lee KR, Hung WS, Wang Z, Li Y, Elimelech M, Jin J, Lin S. Polyamide nanofiltration membrane with highly uniform sub-nanometre pores for sub-1 A precision separation. **Nat. Commun.** 11, 2015-2024 (2020).*'

Response to Reviewer #2

General Comment: The authors discuss the synthesis, membrane preparation and application of ionized sub-nanochannels for ion sieving. The research is new and interesting, of interest to a broad audience. In general, it is well-written and easy to follow, the characterizations are detailed. I recommend publication after addressing the comments below.

Our response to General Comment

We appreciate the reviewer's very encouraging comments. According to your valuable suggestions, we have made modifications as shown below:

Comment #1

The size of the hydrophilic-hydrophobic nanodomains should be indicated in the figure showing the Tröger's base microporous polymer membrane schematic.

Our response to Comment #1

Thank you for your suggestion. We used ImageJ software to calculate the area of hydrophilic and hydrophobic regions in the AFM image (**Fig. 6c**). The results showed that the hydrophilic region accounted for approximately 22.71% and the hydrophobic region for about 77.29%. XPS data **(Supplementary Fig. 4**) further indicated that the degree of quaternization of TB in this work was around 30%. The area ratio of the hydrophilic and hydrophobic regions was consistent with the XPS data. We added the size (ratio) of the hydrophilic and hydrophobic regions to the schematic diagram of Tröger's base microporous polymer membrane (**Fig. 1**).

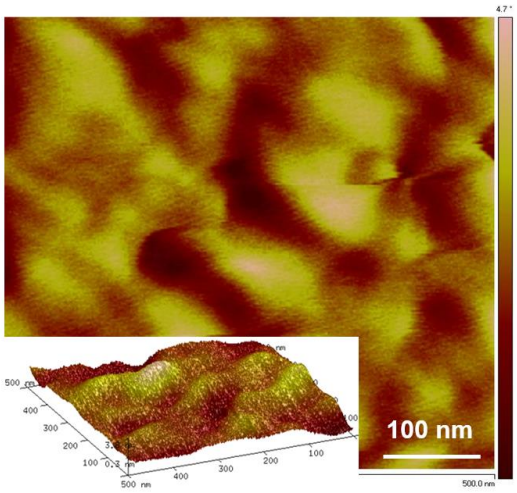

Fig. 6c *Atomic force microscopy (AFM) images of the QA-TB membrane. The bright regions in* ***c*** *represent the hydrophobic segments of the polymer backbone, whereas the dark regions correspond to the hydrophilic portions of the QA groups. The partitioning calculation using ImageJ software reveals that the percentage of hydrophilic region is*

about 22.71% and the percentage of hydrophobic region is about 77.29%.

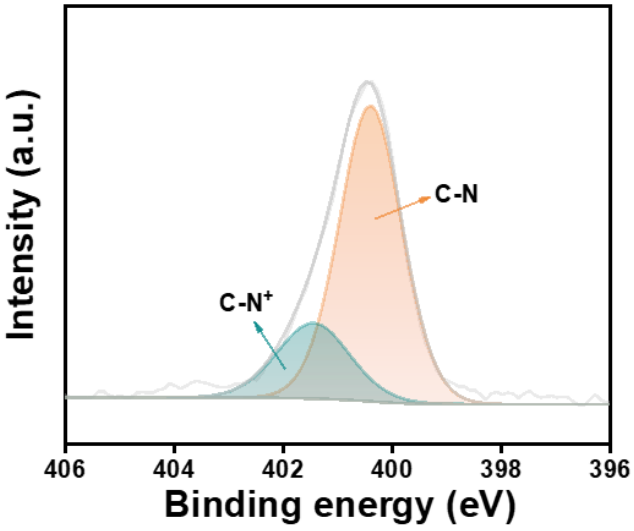

Supplementary Fig. 4 *X-ray photoelectron spectroscopy (XPS) spectra of QA-TB membrane.*

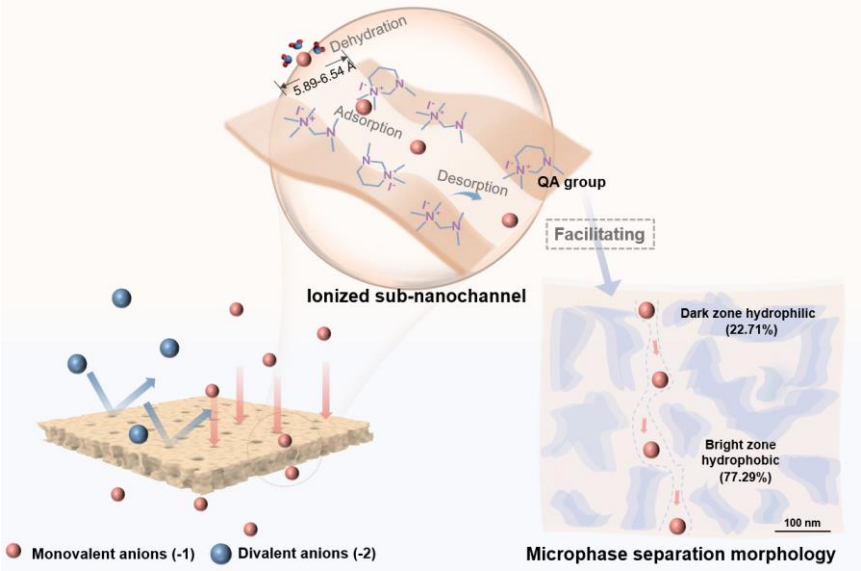

Fig. 1 *Schematic illustration of the Tröger's Base (TB) microporous polymer membrane for ion separations.*

Comment #2

The used monomers are sterically hindered near the reaction site, which usually prevents the polymerization or reduces the yield. The authors could elaborate on these aspects more and discuss how these obstacles were overcome.

Our response to Comment #2

Thank you for your valuable suggestion. The amount of trifluoroacetic acid and the stirring time greatly influence the reaction yield. The polymer yield in this work was

calculated to be 98.45%. Literature reports show that TB polymer yields, based on the polymerization of monomers without steric hindrance near the reaction site, range from 70% to 98% (*J. Am. Chem. Soc.* **144**, 15581-15594 (2022)). This demonstrates that the synthesis conditions we adopted (o-benzidine: dimethoxymethane: trifluoroacetic acid = 1:5.022:26.58) with stirring for 4 days do not hinder polymerization or reduce yield. According to your valuable suggestion, we included the yield in the revised version to help readers understand the polymerization efficiency of this monomer.

*(SI, page 4) 'After that, the solid was filtered, and oven dried at 60℃ for the following synthesis (**98.45% yield**).'*

Comment #3

The radar plot is somewhat difficult to read and therefore the data presented could be also included in the supporting information in a tabulated form.

Our response to Comment #3

Thank you for your suggestion. We have added the detailed characterization data of TB and QA-TB membranes in the **Supplementary Table 2** to enhance clarity for readers, as follows:

Supplementary Table 2 *Properties of the prepared TB and QA-TB membranes.*

Type of membrane	TB	QA-TB
Water Uptake (%)	4.05±0.35	1.75±0.30
Swelling Ratio (%)	0.89±0.13	1.01±0.02
Tensile strength (MPa)	58.15	58.53
Storage modulus (MPa)	1267	1629
Glass transition temperature (°C)	410	338
Zeta potential (mV)	-14	-31
Conductivity ($mS \cdot cm^{-1}$)	7.63	12.23
J_{Cl} ($\times 10^{-4} \cdot mol \cdot m^{-2} \cdot s^{-1}$)	4.07	16.13
Mw ($g \cdot mol^{-1}$)	74826	76108
Intrinsic viscosity ($dL \cdot g^{-1}$)	0.81	1.06

Comment #4

The degree of methylation as well as the molecular weight of the polymer should be determined because it is an important factor influencing the membrane performance.

Our response to Comment #4

Thank you for your valuable suggestion. The weight average molecular weights of TB and QA-TB polymers are 74,826 and 76,108 g mol^{-1}, respectively. And the intrinsic viscosities of them are 0.81 and 1.06 dL g^{-1}, respectively. They are sufficient to meet the preparation conditions for polymer membranes. Additionally, XPS results indicate that the degree of quaternization is approximately 30% (area ratio of C-N^+ to C-N). The appropriate degree of quaternization avoids the increase of membrane brittleness and the decrease of mechanical strength caused by hydrophilic quaternary ammonium groups, while ensuring sufficient adsorption sites in the ionized sub-nanochannels to promote ion migration. We have included the degree of quaternization and molecular weight information of the polymers in the SI, as follows:

(SI, page 3) 'Gel Permeation Chromatography (GPC, Shimadzu LC-20A, Japan) was used to test the molecular weight of polymers by completely dissolving TB and QA-TB polymers in the N-methyl pyrrolidone. X-ray photoelectron spectroscopy (XPS, Thermo Fisher Scientific, USA) was used to observe the quaternization degree of membranes.'

*(SI, page 4) '**Intrinsic viscosity**. The intrinsic viscosity ([ŋ]) of the polymers was measured using a Schott Viscometry System (AVS 370, Germany) in a DMSO solution at 25℃. The Schott Viscosystem (AVS 370, Germany) was composed of an Ubbelohde viscometer (SI Analytics, Type 530 13: Capillary No. Ic, K = 0.03) and automatic piston burette (TITRONIC universal). First, a target sample was dissolved in DMSO to form a 3 mg mL^{-1} polymer solution. Then, the solution was automatically diluted into five concentrations in order (3.0, 2.5, 2.0, 1.5, and 1.0 mg mL^{-1}), and five efflux times were recorded. The intrinsic viscosities ([ŋ]) of polymers could be calculated from the following equation:*

$$\eta = \frac{\ln(\frac{t_s}{t_b})}{c}$$

where t_s (s) and t_b (s) are the efflux time of DMSO and the polymer solution, respectively, c (g dL^{-1}) is the concentration.'

Supplementary Table 2 *Properties of the prepared TB and QA-TB membranes.*

Type of membrane	TB	QA-TB
Water Uptake (%)	4.05±0.35	1.75±0.30
Swelling Ratio (%)	0.89±0.13	1.01±0.02
Tensile strength (MPa)	58.15	58.53
Storage modulus (MPa)	1267	1629
Glass transition temperature (°C)	410	338
Zeta potential (mV)	-14	-31
Conductivity ($mS\ cm^{-1}$)	7.63	12.23
J_{Cl} ($\times 10^{-4}\ mol\ m^{-2}\ s^{-1}$)	4.07	16.13
Mw ($g\ mol^{-1}$)	74826	76108
Intrinsic viscosity ($dL\ g^{-1}$)	0.81	1.06

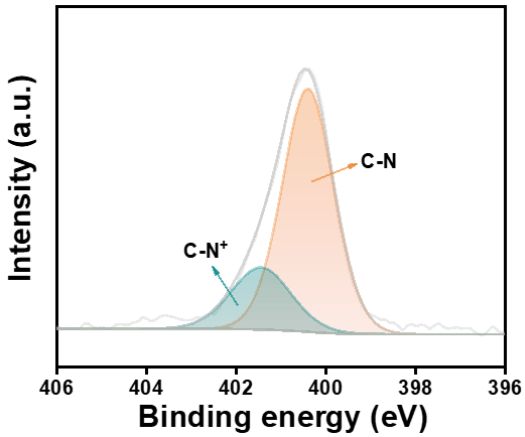

Supplementary Fig. 4 *X-ray photoelectron spectroscopy (XPS) spectra of QA-TB membrane.*
Note: The appearance of the C-N⁺ peak confirms successful quaternization of the TB membrane. Comparing the peak areas of C-N⁺ and C-N revealed that the degree of quaternization of TB is approximately 30%. This degree of quaternization avoids excessive hydrophilic quaternary ammonium groups that increase membrane brittleness and reduce mechanical strength, while ensuring sufficient adsorption sites in the ionized sub-nanochannels to promote ion migration.

Comment #5

The ion separation performance of the membranes should be compared with the state of the art membranes in the literature.

Our response to Comment #5

Thank you for your suggestion. We have included the latest literature for comparing the membrane performance and found that the anions separation performance of the QA-TB membrane far exceeds those reported in the literature (**Fig. 4e and Supplementary Table 3**).

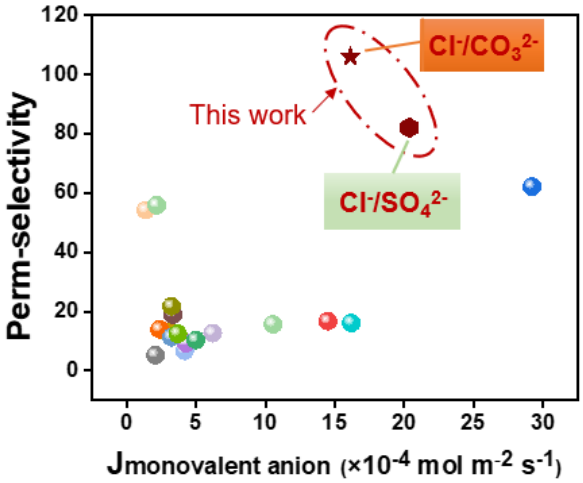

Fig. 4e *Comparison of monovalent and divalent anion separation performance of QA-TB membrane with previously reported membranes.*

Supplementary Table 3 *Comparison of monovalent and divalent anion separation performance of QA-TB membrane with previously reported membranes.*

Type of membranes	Separation system	Monovalent anion flux ($\times 10^{-4}$ mol m^{-2} s^{-1})	Permeation selectivity	Reference
PAES-UIO-66-Pyr	Cl^-/SO_4^{2-}	1.4	54.26	16
QDPAB-C7	Cl^-/SO_4^{2-}	10.56	15.7	17
HPABP-CC3(15)	Cl^-/SO_4^{2-}	6.22	12.67	18
QP-P3-1	Cl^-/SO_4^{2-}	4.2	6.7	19
QP-P6-1	Cl^-/SO_4^{2-}	4.3	9.3	19
QP-P11-1	Cl^-/SO_4^{2-}	3	13.07	19
PPO-0.100-ImPS	Cl^-/SO_4^{2-}	16.2	16.12	20
sCOF/aAEM3	Cl^-/SO_4^{2-}	3.35	18.92	21
Blend-15 AIEM	Cl^-/SO_4^{2-}	3.25	21.8	22
Blend-10 AIEM	Cl^-/SO_4^{2-}	2.4	14	22
Blend-0 AIEM	Cl^-/SO_4^{2-}	3.25	11.3	22
PAES-im-2.5c AIEM	Cl^-/SO_4^{2-}	3.7	12.5	23
Neosepta ACS	Cl^-/SO_4^{2-}	2.1	5.27	23
MQ18	Cl^-/SO_4^{2-}	14.5	16.7	24
AF1-HNN5-50	Cl^-/SO_4^{2-}	29.2	62.2	25
PQC76/DSA-0.5	Cl^-/SO_4^{2-}	5	10.38	26
PAES-UIO-66-Py	NO_3^-/SO_4^{2-}	2.19	55.9	16
QA-TB	Cl^-/SO_4^{2-}	20.37	82	This work
QA-TB	Cl^-/CO_3^{2-}	16.13	106	This work

Response to Reviewer #3

General Comment: This study introduced randomly twisted V-shaped Tröger's Base units and quaternary ammonium groups to construct ionized sub-nanochannel membranes. By combining size sieving and electrostatic interactions, the membranes demonstrated impressive selectivity for separating monovalent and divalent anions. The results represent significant breakthroughs and have broad interest, with a comprehensive and reasonable separation mechanism. Therefore, the study is suitable for publication in Nature Communications with minor revisions suggested. Specific comments are listed below:

Response to General Comment

We are grateful for the positive evaluation of our work. According to your valuable suggestions, we have made modifications as shown below:

Comment #1

The authors proposed in the abstract section that the V-shaped structure of TB unit with quaternary ammonium groups constructs ionized sub-nanochannels. Polymer membranes are usually described as possessing ion channels or transport channels, so the authors could describe in detail what is meant by ionized sub-nanochannels.

Our response to Comment #1

Thank you for your suggestion. The term "ion/transport channel" typically describes ion migration pathways in membrane micropores but lacks specificity. We define the micropores in TB membranes as ionized sub-nanochannels. The TB unit provides a sub-nanochannel (or transport channels as reviewer mentioned), whereas the quaternary ammonium group provides ion adsorption sites, and the introduction of counterions promotes the migration of target ions, ultimately forming the ionized sub-nanochannel. We explain the ionized sub-nanochannel in the legend of **Fig. 1** for clarity.

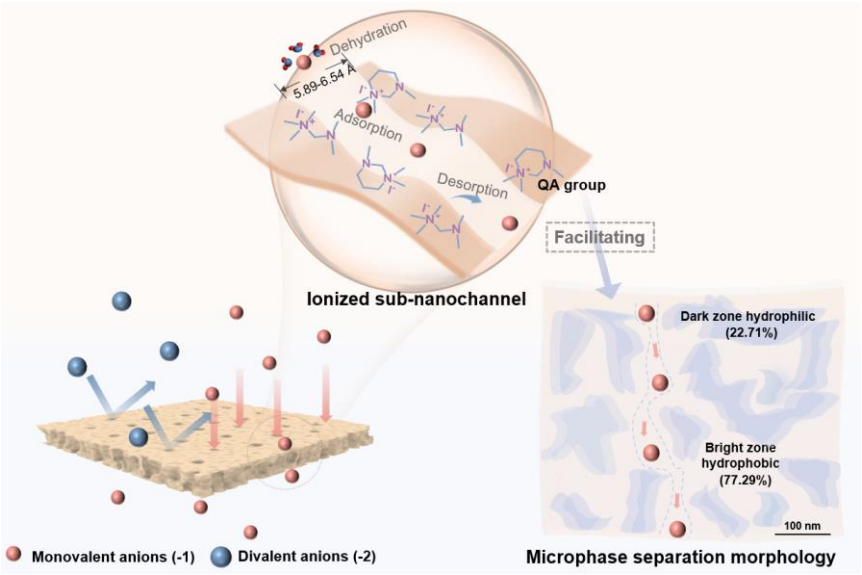

Fig. 1 Schematic illustration of the Tröger's Base (TB) microporous polymer membrane for ion separations. *Ionized sub-nanochannels were engineered through the strategic integration of angstrom-porous quaternized TB units with ion adsorption sites.* The randomly twisted V-shaped structure of TB provides regulated membrane pores with a pore window size of 5.89-6.54 Å, positioned between the anion hydration diameter and their Stokes diameter. Additionally, the incorporation of functional groups (quaternary ammonium groups) promoted channel-ion interactions and improved the monovalent ion flux.

Comment #2

"Although a minimal migration of CO_3^{2-} was observed within the final 35 minutes, amounting to less than one-fifth of the migration of Cl^-, it remained relatively steady (Fig. 3b)." This is an interesting experimental phenomenon. Are there any potential reasons that the authors could provide?

Our response to Comment #2

Thank you for your suggestion. This phenomenon is mainly due to the difference in the migration rates of Cl^- and CO_3^{2-}. Cl^- has lower dehydration energy and smaller size than CO_3^{2-}. This allows Cl^- to dehydrate and migrate rapidly under an electric field, leading to its gradual accumulation over time. CO_3^{2-} has higher binding energy with water molecules and stronger adsorption energy within the channel, making its dehydration and desorption more challenging. The size of ionized sub-nanochannel cannot facilitate the migration of hydrated ions (**Fig. 5b**), thus hindering initial ion migration of CO_3^{2-}. Over time, as ions gradually dehydrate and desorb, a minor migration of CO_3^{2-} is observed. However, its migration rate is still much lower than that of Cl^-. In the following section ***Unveiling separation mechanisms: ion dehydration, microphase separation, and ion interactions***, we detailed the mechanisms of the differences in migration rates. Here, we have also briefly explained, as follows:

（main text, Page 9） *'Although a minimal migration of CO_3^{2-} was observed within the final 35 minutes, amounting to less than one-fifth of the migration of Cl^-, it remained relatively steady (**Fig. 3b**). Because CO_3^{2-} exhibits greater dehydration difficulty and consequently migrates more slowly than Cl^- ions, especially when hydrated.'*

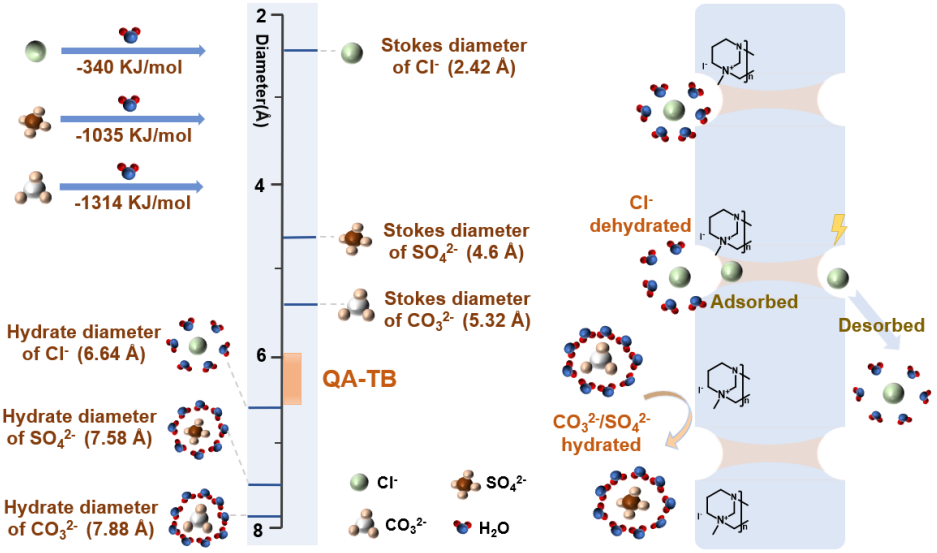

Fig. 5b Schematic illustration of the separation mechanisms for monovalent (Cl^-) and divalent (CO_3^{2-}, SO_4^{2-}) anions, considering the influence of hydration energy and size of anions.

Comment #3

"The migration of Cl^- in one hour was markedly higher than that of SO_4^{2-} (Supplementary Fig. 7), achieving a Cl^- flux of 20.37×10^{-4} mol m^{-2} s^{-1} and a permeation selectivity of 82 (Supplementary Fig. 8). The ion migration rate was even faster than that in the Cl^-/CO_3^{2-} system, with complete Cl^- migration achieved within 48 hours (Supplementary Fig. 9), while the optimal permeation selectivity was slightly lower." In this article, the membrane constructed all showed high ion fluxes and permeation selectivity in the ion separation process. Why the ion flux is lower in the Cl^-/CO_3^{2-} system but the selectivity is higher?

Our response to Comment #3

Thank you for your comment. CO_3^{2-} undergoes hydrolysis, producing HCO_3^- which competes with Cl^- for migration in solution, thereby reducing the Cl^- flux below that of the Cl^-/SO_4^{2-} system. However, the degree of hydrolysis of CO_3^{2-} is extremely low (the maximum concentration of HCO_3^- is 8×10^{-5} mol L^{-1}), and it mainly exists in the form of CO_3^{2-} in the solution (**Supplementary Fig. 8**). Due to its larger size and higher hydration free energy compared to Cl^- and SO_4^{2-}, CO_3^{2-} exhibits the slowest dehydration migration rate. This exceptionally slow migration rate contributes to its high selectivity for separation from Cl^-. We changed the related description in the revised manuscript, as follows:

（main text, pages 13-14） *'The ion migration rate was even faster than that in the Cl^-/CO_3^{2-} system, with complete Cl^- migration achieved within 48 hours (**Supplementary Fig. 11**), while the optimal permeation selectivity was slightly lower ($P_{SO_4^{2-}}^{Cl^-} = 82 < P_{CO_3^{2-}}^{Cl^-} = 106$). This difference arises from that a small amount of HCO_3^- initially reduces the Cl^- flux, while CO_3^{2-} has larger size and higher hydration free energy compared to Cl^- and SO_4^{2-}. Consequently, CO_3^{2-} dehydrates and migrates at the slowest rate, resulting in higher selectivity for separation from Cl^-.'*

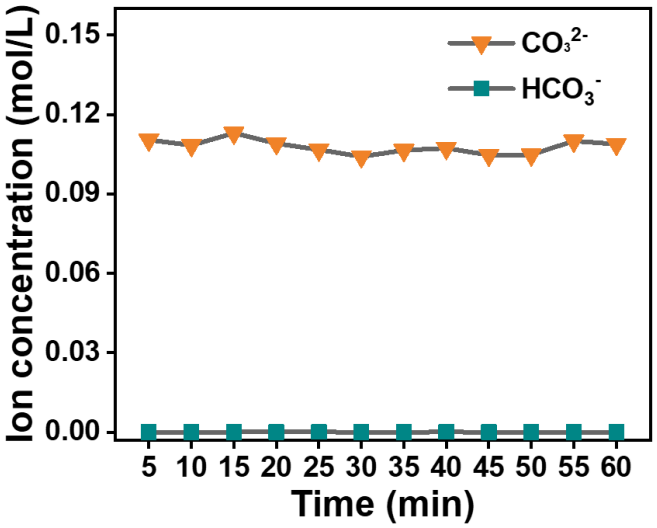

Supplementary Fig. 8 Ion concentrations of CO_3^{2-} and HCO_3^- in the dilution chamber.

Comment #4

"However, the Cl^- and SO_4^{2-} separation performance of the QA-TB membrane far exceeded those reported in the literature (Fig. 4e)." The authors compared the performance of the fabricated membranes with data from seven references. Suggesting the authors to compare the data with more literature.

Our response to Comment #4

Thank you for your suggestion. We have included the latest literature for comparing the membrane performance and found that the anions separation performance of the QA-TB membrane is still at the optimal value for those reported in the literature (**Fig. 4e** and **Supplementary Table 3**).

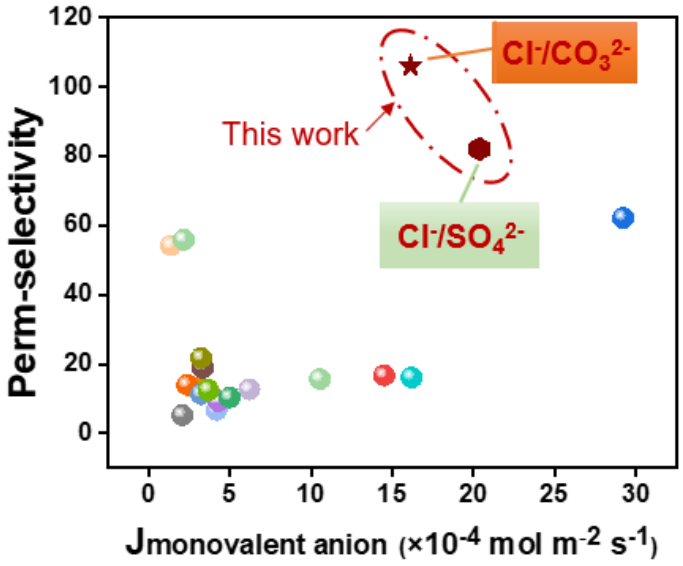

Fig. 4e Comparison of monovalent and divalent anion separation performance of QA-TB membrane with previously reported membranes.

Supplementary Table 3 Comparison of monovalent and divalent anion separation performance of QA-TB membrane with previously reported membranes.

Type of membranes	Separation system	Monovalent anion flux ($\times10^{-4}$ mol m^{-2} s^{-1})	Permeation selectivity	Reference
PAES-UIO-66-Pyr	Cl^-/SO_4^{2-}	1.4	54.26	16
QDPAB-C7	Cl^-/SO_4^{2-}	10.56	15.7	17
HPABP-CC3(15)	Cl^-/SO_4^{2-}	6.22	12.67	18
QP-P3-1	Cl^-/SO_4^{2-}	4.2	6.7	19
QP-P6-1	Cl^-/SO_4^{2-}	4.3	9.3	19
QP-P11-1	Cl^-/SO_4^{2-}	3	13.07	19
PPO-0.100-ImPS	Cl^-/SO_4^{2-}	16.2	16.12	20
sCOF/aAEM3	Cl^-/SO_4^{2-}	3.35	18.92	21
Blend-15 AIEM	Cl^-/SO_4^{2-}	3.25	21.8	22
Blend-10 AIEM	Cl^-/SO_4^{2-}	2.4	14	22
Blend-0 AIEM	Cl^-/SO_4^{2-}	3.25	11.3	22
PAES-im-2.5c AIEM	Cl^-/SO_4^{2-}	3.7	12.5	23
Neosepta ACS	Cl^-/SO_4^{2-}	2.1	5.27	23
MQ18	Cl^-/SO_4^{2-}	14.5	16.7	24
AF1-HNN5-50	Cl^-/SO_4^{2-}	29.2	62.2	25
PQC76/DSA-0.5	Cl^-/SO_4^{2-}	5	10.38	26
PAES-UIO-66-Py	NO_3^-/SO_4^{2-}	2.19	55.9	16
QA-TB	Cl^-/SO_4^{2-}	20.37	82	This work
QA-TB	Cl^-/CO_3^{2-}	16.13	106	This work

Comment #5

"Meanwhile, different degrees of interaction between the QA-TB framework and ions help ions with different free energies and transfer along the pore walls at different speeds." What does "interaction" mean? Please give a specific explanation.

Our response to Comment #5

Thank you for your comments. The interaction between the QA-TB framework and ions is primarily electrostatic, involving both attraction and repulsion. As we have described in the Abstract 'Combining the size sieving and electrostatic interaction effects, sub-nanochannel membranes achieved exceptional ion selectivity of 106 for Cl^-/CO_3^{2-} and 82 for Cl^-/SO_4^{2-}, significantly surpassing those of the state-of-the-art membranes. Meanwhile, the adsorption and desorption energies of ions at QA-TB adsorption sites were calculated, comparing the interaction strengths of different ions (**Fig. 6d**). We changed the related description in the revised manuscript, as follows:

（main text, page 14）'*Meanwhile, different degrees of* ***electrostatic interaction*** *between the QA-TB framework and ions help ions with different free energies and transfer along the pore walls at different speeds.*'

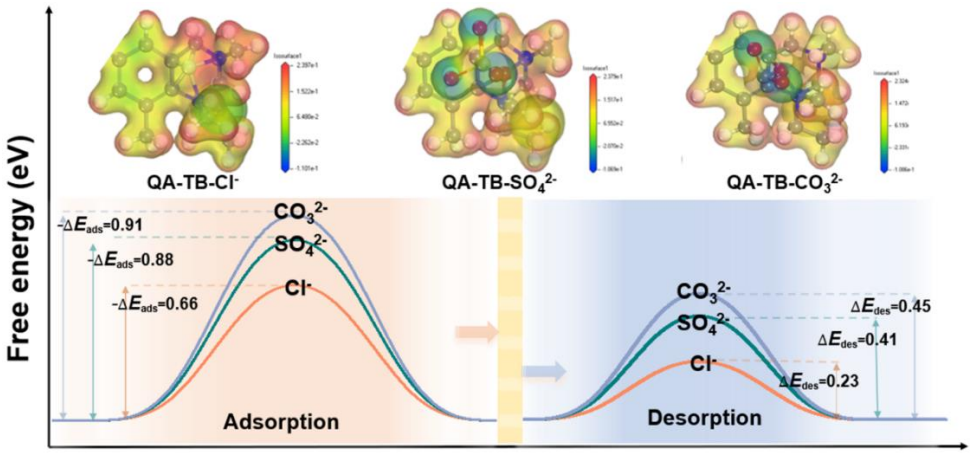

Fig. 6d Electrostatic potential diagrams and calculations of adsorption and desorption energies for $Cl^-/SO_4^{2-}/CO_3^{2-}$ on the surface of QA-TB. The CO_3^{2-} exhibits greater negative adsorption energy, indicating stronger adsorption to QA-TB, and has higher desorption energy, hindering desorption. Conversely, Cl^- shows the lowest free energy, resulting in faster migration.

Reviewers' Comments:

Reviewer #1:
Remarks to the Author:
The authors have addressed the questions and comments raised by the reviewers, resulting in revisions and improvements to the manuscript. However, there is a minor revision suggestion: In Supplementary Fig. 5, the electron micrograph is unclear and should be replaced with better-focused images to demonstrate that quarterization does not affect the surface morphology.

Reviewer #2:
Remarks to the Author:
After checking the response letter and the changes to the manuscript, I support the publication of the manuscript as is.

Reviewer #3:
Remarks to the Author:
The authors have well responded the comments, and this manuscript now can be accepted for publication.

Response to Reviewers' Comments

Response to Reviewer #1 (Remarks to the Author):

General Comment: The authors have addressed the questions and comments raised by the reviewers, resulting in revisions and improvements to the manuscript. However, there is a minor revision suggestion: In Supplementary Fig. 5, the electron micrograph is unclear and should be replaced with better-focused images to demonstrate that quaternization does not affect the surface morphology.

Our response to General Comment

We appreciate the reviewer's careful evaluation of our work. We updated the electron microscopy images and replaced them with better-focused images. It could be found that quaternization does not affect surface morphology.

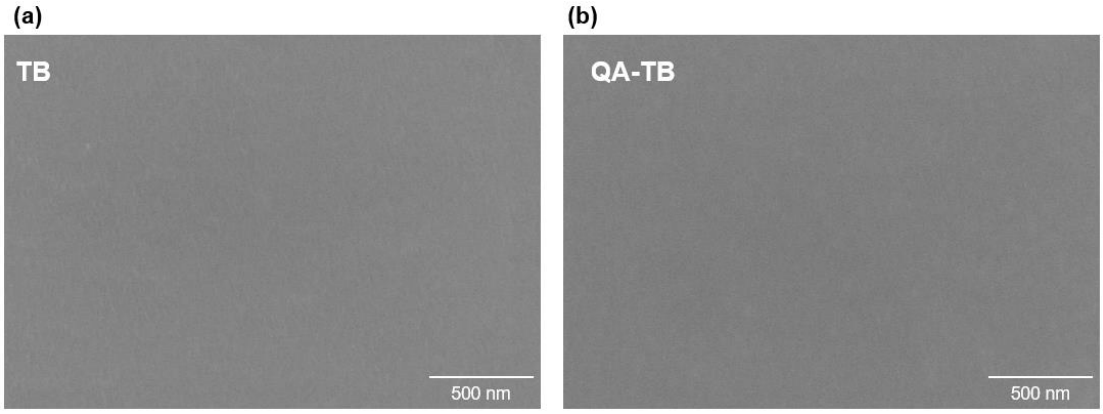

Supplementary Fig. 5 Surface morphologies of (a) TB and (b) QA-TB membranes.